Surface deformation detected by the space-observed small baseline SAR interferometry over permafrost environment of Beiluhe section, Hoh Xil natural reserve in Tibet Plateau, China

Fulong Chen[a,b], Hui Lin[b]*

[a] Institute of Remote Sensing and Digital Earth, Chinese Academy of Sciences, No.9 Dengzhuang South Road, Haidian District, Beijing 100094, China;

[b] Institute of Space and Earth Information Science, The Chinese University of Hong Kong, Shatin, N.T., Hong Kong, China.

*Corresponding author. Tel.: +852 3943 6010; fax: +852 2603 7470.

E-mail addresses: huilin@cuhk.edu.hk (H. Lin); chenfulong@ceode.ac.cn (F. Chen).

Abstract: The evolution of permafrost and the active layer is highly related to biological diversity and climate change because of its feedback effects involving water and carbon storage. In this study, we firstly examined the relationship of active layer variation, geomorphological process and anthropogenic activities by means of small baseline synthetic aperture radar interferometry in Beiluhe, Hoh Xil natural reserve in Tibet Plateau (TP), China, using 3.5-yr observation span of L-band ALOS PALSAR data (June, 2007 to December, 2010). The estimated surface displacements (primarily in the range of -30 mm yr^{-1} to 30 mm yr^{-1}) and time-series implied evolutions of the active layer and permafrost beneath. The motion trend along slopes was complicated due to the geomorphological process, and thus interdisciplinary interpretations were required. Anthropogenic influences on this frail permafrost environment were significant, proved by the remarkable surface settlement along the embankment of Qinghai-Tibet Railway. Consequently, it is crucial and necessary to monitor this permafrost plateau owing to the combination of climate change, geo-hazards prediction, natural reserve conservation as well as the regional sustainable development.

Keywords: Small BAseline Subsets; permafrost; Tibet Plateau; Qinghai-Tibet Railway; natural reserve;

1. Introduction

The Tibet Plateau (TP), recognized as the third pole of Earth, has the largest permafrost extent outside the polar region (Chen et al., 2012b). Permafrost is sensitive to global warming, resulting in significant influences on regional water balance, biological diversity, carbon cycle and engineering constructions. TP, known as the Asia water tower, is the source region of many major rivers in Asia (Immerzeel et al., 2008). The perennial flow of those rivers largely relies on the constant flux from glaciers melting. Approximately 23-48% of the total global soil carbon pool is stored in permafrost regions in the world (Guo and Macdonald, 2006; Tarnocai et al., 2008). Alpine permafrost in TP bears a greater organic carbon pool than do grassland soils in other regions of China (Wang et al., 2008). Thus carbon emission from permafrost has been highly concerned when it thaws under global warming (Monastersky, 2011; Schuur et al., 2008). The active layer overlaid on permafrost tends to be instable determined by the dynamics of frost heave and thaw settlement. As the plateau is being developed, the anthropogenic activities, such as expansive natural resource exploitation and tourism, have introduced external pressures to the local environment and biological diversity. All issues described above are closely correlated with the dynamics of the active layer as well as beneath permafrost, e.g. growth or degradation.

As the highest terrestrial unit, abundance of studies has been conducted in TP because of its significance for global and regional sustainable development, including climate change and carbon emission (Liu et al., 2009; Wu et al., 2010), tectonics and earthquake (Ismail-Zadeh et al., 2007; Loveless and Meade, 2011; Qiao et al., 2011), water balance (Niu et al., 2011; Wang et al., 2009a,b) and permafrost environment (Jin et al., 2008; Wu and Zhang, 2008, 2010; Yang et al., 2004). However, the estimation of surface movements over permafrost environment, particularly in TP, using spaceborne Synthetic Aperture Radar Interferometry (InSAR) (Chen et al., 2012b) is still inadequate. Differential InSAR (DInSAR) (Massonnet et al., 1993), one of the quantitative remote sensing technologies, has proved to be effective for ground motion detection by measuring the phase difference of two or multi-temporal SAR acquisitions (Chen and Lin, 2011; Hooper et al., 2012). The development of Multi-Temporal SAR Interferometry (MT-InSAR), which mitigates the intrinsic limitations of the traditional DInSAR (spatial-temporal decorrelation as well as atmospheric disturbance); and thus is capable of deriving surface motion rates with millimetric accuracy using large datasets over the same area. In general, MT-InSAR can be divided into two main categories, including Persistent Scatterer (PS) (Ferretti et al., 2000; Hooper et al., 2004) and Small BAseline Subsets (SBAS) (Berardino et al., 2002; Chen et al., 2010, 2012a; Jiang et al., 2011; Lanari et al., 2004; Lin et al., 2011). The former concentrates on the phase analysis of PS points using single reference interferogram formation; in contrast, the alternative prefers to extract information from distributed scatterer (DS) points with the aid of multi-references interferogram formation based on the small baseline constraint.

The past investigation demonstrated that, in the permafrost environment of TP, the DS points are prevalent except for the artificial structures, e.g. the embankment of Qinghai-Tibet Railway (QTR) (Chen et al., 2012b). Consequently, in order to extract information as much as possible, the SBAS is introduced for the evolution analysis of the active layer and permafrost. In total, 19 L-band ALOS PALSAR SLC images (acquired from June 2007 to December 2010) are employed to cover the Beiluhe experimental site, Hoh Xil natural reserve in TP of China. The subsequent sections will be organized as follows: In Sect. 2, the study site and data are firstly described. Then, a re-call SBAS methodology and its corresponding procedures are shown in Sect. 3 for easily understanding. After that, the SBAS derived results are shown and then interpreted in Sect. 4. Taking natural slopes and the QTR as instances, Sect. 5 shows the discussion of surface displacements with respect to permafrost environments, geomorphological processes as well as anthropogenic activities. Finally, some conclusions are drawn.

2. Study area and datasets

For the easy accessibility and available ground-based measurements, the Beiluhe, Hoh Xil natural reserve, TP of China is selected as the experimental site (see Fig.1), approximately extending from 92° 16′ to 93° 1′ E and from 34° 5′ to 34° 55′ N. The temporal averaged amplitude SAR image in Fig. 1 shows the study site coverage with a spatial extent of 63×45 km^2 approximately. The QTR can be easily indentified due to its strong backscattering characteristic, as marked by the pink line (the dotted section indicates the Fenghuo Mount Tunnel). The topography of this site is composed by upland in the middle section in NW-SE direction represented by Fenghuo Mount, Ri'achi Mount; and mild terrain in the northeast and southwest represented by Beiluhe valley and Erdaogou valley. The arid continental climate is prevailing due to the high elevation (from 4500 to 5200 m). Compared with the scarce precipitation (approximately 300-400 mm yr^{-1}), the evaporation is about 2-3 times higher, resulting in arid condition owing to the negative water budget. However, warm and ice-rich permafrost (WIRP) is well developed in several sub-regions, particularly surrounding the above two valleys with mild terrain, high soil moisture as well as relatively warm ground temperature (-1.8 to -0.5℃). Generally, compared with mountainous regions, the sub-surface temperature and ice-content of the active layer and permafrost beneath are both higher in mild-terrain valley terraces; thawing islands could even exist through WIRP regions in case of the occurrence of rivers and geothermal heat flows.

19 ALOS PALSAR images acquired with ascending orbit and 34.3-degree nominal radar look angle, from June 2007 to December 2010, were used in this study, including 9 scenes of Fine Beam Single polarization (FBS, 28 MHz) and 10 scenes of Fine Beam Dual polarization (FBD, 14 MHz). Interested readers can refer to Chen et al., (2012b) for more details. The ALOS PALSAR data were obtained from the Japan Aerospace Exploration Agency (JAXA). In general, ALOS PALSAR has two advantages for the TP region monitoring: firstly, PALSAR works with a longer wavelength (L-band, 23.6 cm), enabling to better penetrate vegetation and resulting in high quality interferograms; secondly, the ground resolution of PALSAR (8 m of FBS and 16 m of FBD) is higher than other median resolution data (e.g. 25-30 m of ERS-1/2 and Envisat ASAR), and thus preserves more detailed information. For the topographical data, 3-arcsecond Shuttle Radar Topography Mission (SRTM) DEM data from the United States Geological Survey (USGS) were applied, firstly for the topographic phase removal in DInSAR procedures, and then for InSAR products geocoding.

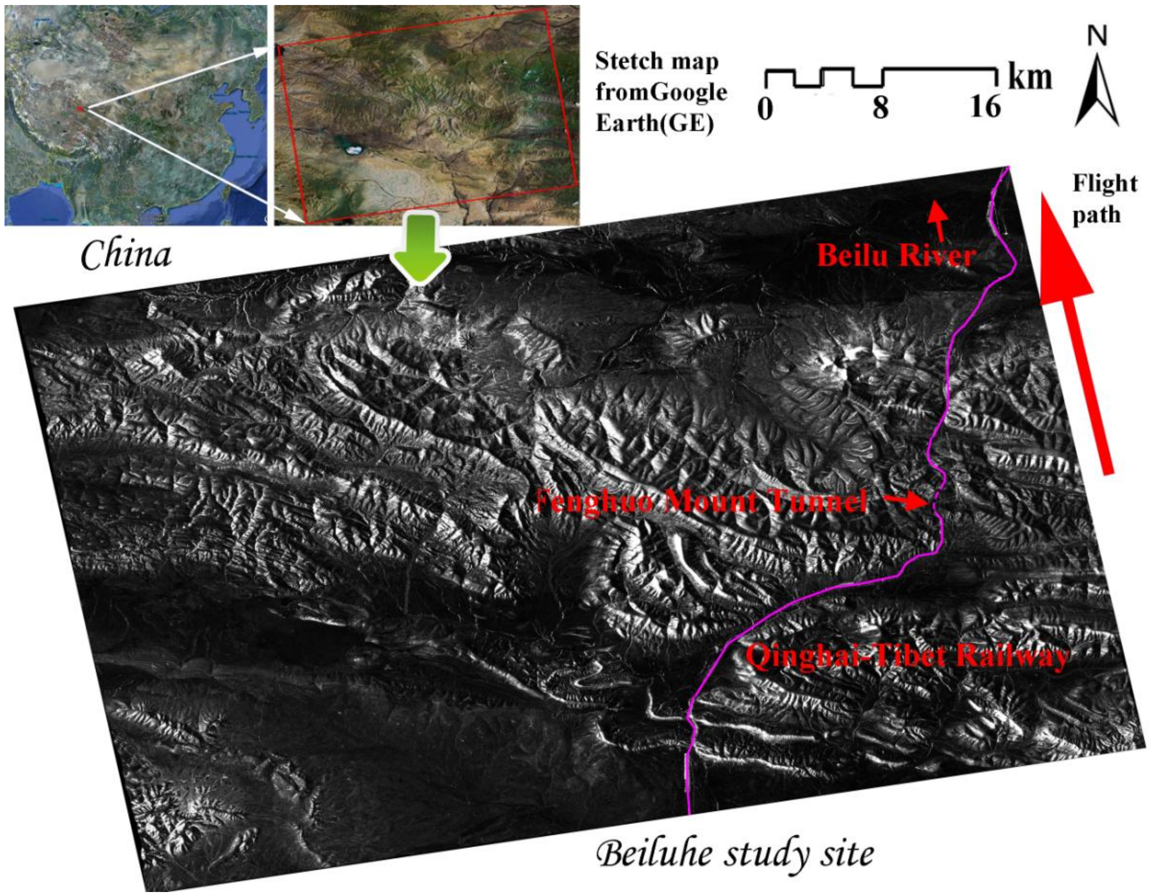

Fig. 1. Location of Beiluhe, Hoh Xil natural reserve in TP of China. The Qinghai-Tibet Railway is marked by the pink line (dotted section indicates the Fenghuo Mount Tunnel). ALOS PALSAR flight path is marked by the red arrow, and the optical inset images are from the Google Earth (GE).

3. SBAS procedures

Inspired by previous investigations (Rykhus and Lu, 2008; Short et al., 2011), InSAR measurements were introduced for surface deformation monitoring over permafrost environment in Beiluhe section, Hoh Xil natural reserve of TP. We found that the seasonal effect and non-linear surface motions in this arid region are evident (Chen et al., 2012b). Except for geomorphological process in slope regions, we hypothesized that the surface deformation diving-force of TP is analogous to Alaska, USA as described by Liu et al. (2010, 2012), that is, the surface movements are caused by two primary components: seasonal displacement by thaw settlement or frost heave of the active layer, and the secular subsidence due to thawing of ice-rich permafrost near the permafrost table. Our past field investigations indicated that apart from artificial structures, e.g. QTR, DS features are dominant over Hoh Xil natural reserve in TP. Consequently, in order to extract surface motions (geomorphological process, the combination dynamics of permafrost and the overlaid active layer), in this study, the SBAS method (Berardino et al., 2002) is introduced taking advantages of its capability of dense DS extraction.

In the SBAS approach, interferogram formation is controlled by thresholds of spatial-temporal baselines as well as the Doppler centroid difference. In this study, only the spatial-temporal baselines are applied (small than 3800 m spatially and 368 days temporally), because of the negligible difference of Doppler centroids. The common HH polarization data from two fine modes are used for interferometric processing after the FBS data are doubly down-sampled in range direction. The multi-looking with 1 by 5 in range and azimuth direction are used to derive InSAR products with approximately 16 m ground resolution. Then initial 67 differential interferograms are generated (note that the topographic and flat earth phase components have been removed). The Minimum Cost Flow (MCF) (Colesanti, 1998) is used for phase unwrapping. After careful checking by manual, another 7 low-quality interferograms (including phase unwrapping errors or significant ionospheric component of atmosphere) are discarded to derive 60 final interferograms for further motion estimation and time series analysis, as illustrated in Fig. 2. It is clear that the PALSAR perpendicular baseline is correlated with the time of acquisition (Samsonov, 2010), implying the suitability of SBAS method for the TP investigation in the case of isolated interferogram subsets in time. In addition, taking advantages of SBAS, the small baseline formation further mitigates topographic errors before parameters (e.g. residual height, displacements and atmospheric disturbance) inversion.

In general, the implementation of SBAS is comprised of two main steps. The first step is the estimation of low-pass displacement and residual height using a preferred cubic displacement model. The Coherent Point (CP) candidates are characterized by a high average spatial coherence. The CP with the maximum value is selected as the reference point. In this step, the Least Squares (LS) algorithm is applied for parameters inversion. The second step is concentrated on the displacement time series retrieval and atmospheric artifacts isolation. That is, a) we derive residual phases by subtracting the low-pass component signatures (derived in the first step) from the original differential interferograms; b) we unwarp residual phases, and then calculate the improved interferogram phases by adding back the previous low-pass components; c) we estimate motion time series using the Singular Value Decomposition (SVD) algorithm; d) we derive refined residual phases by subtracting the low-pass deformation component from the motion time series; e) we estimate atmospheric artifact phases using temporal-spatial filters (firstly a temporal high-pass and then a spatial low-pass); f) we derive the final deformation components after the atmospheric artifacts isolation. Note that final CPs are further identified by the temporal coherence with respect to a defined displacement model.

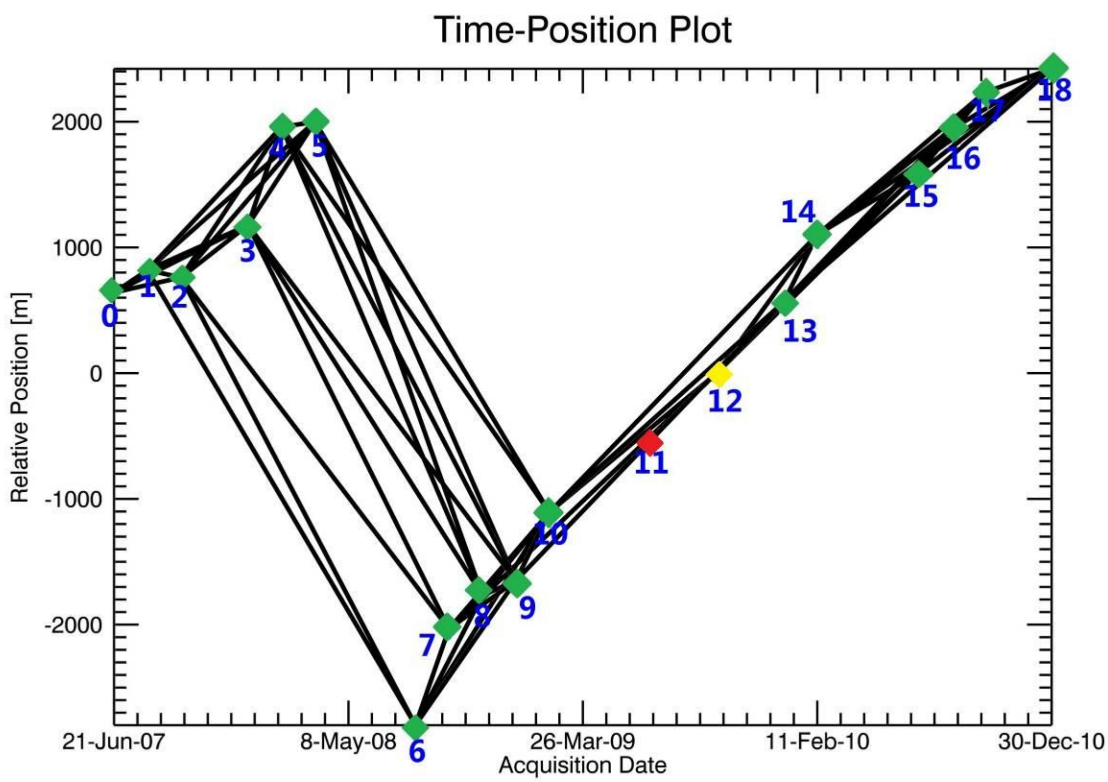

Fig. 2. Spatial-temporal distribution of interferogram formation based on the small baseline constraint. It is clear that the perpendicular baselines are correlated with the acquisition time. The number 12 image marked in yellow is the reference image acquired on 26 September 2009 for the dataset co-registration. The image marked in red is discarded because of its evident atmospheric disturbance.

4. Results, validation and monitoring interpretation

Using the two thresholds (0.4 average spatial coherence and 0.6 temporal coherence), the SBAS derived surface displacement rates in line-of-sight (LOS) over Beiluhe section, Hoh Xil natural reserve of TP are illustrated in Fig. 3. The negative motion rates' sign is indicative of an increasing distance with time away from the satellite (subsidence); and positive sign represents an uplift motion. The result indicates that the surface motion in permafrost environment is evident, primarily in the range of -30 mm yr^{-1} to 30 mm yr^{-1} in the 3.5-yr observation span (from June, 2007 to December, 2010). The InSAR-derived results have been validated by leveling data located nearby the Fenghuo Mount Tunnel frontier (marked by the cross in Fig. 3). The two different types of data demonstrate consistent motion trends with absolute discrepancies varying from 0.5 to 4 mm yr^{-1} (please refer to Chen et al., 2012b for more details). There are totally 8025313 CPs over the study site with approximately 63×45 km^2, that is, 2800 CPs km^{-2}. The high spatial density of CPs is determined by following two aspects. Firstly, PALSAR has a long wavelength, resulting in high penetration and coherence preservation, particularly in non-urban areas, e.g. TP. Second, the small baseline strategy is introduced in interferometric formation, and thus high-quality interferograms can be guaranteed, resulting in high spatial density of CP candidates and then the final CPs.

In order to interpret the motion trends (magnitude and direction), particularly for slope regions, the relationship between SAR imaging geometry (ascending with 34.3 degree looking angle in this case) and the surface displacement is analyzed (see Fig. 4). With a few exceptions, the direction of surface movements holds the following assumption: the parallel movement, caused by the shallow-seated landslides, is dominant in the middle section of slopes; vice versa, for other portions, landslides are rare and the rotational motion is prevalent caused by the alluvial accumulation or the combination dynamics of permafrost and the overlaid active layer, such as the secular subsidence due to ice-rich permafrost thawing near the permafrost table. That is, in the upper section of slopes, the rotational motions from both sides demonstrate consistent movements: frost heave as uplifts in LOS and thaw settlement as subsidence in LOS, as marked by 'a' , 'aa' and 'b', 'bb'. For the slope facing the satellite, the downslope movement of material on the steep section (angle of gradient > 34.3 degree) demonstrates as mild subsidence (marked by 'c_1') and on the moderate section (angle of gradient < 34.3 degree) demonstrates as mild uplift (marked by 'c_2'); in contrast, those two motion components both demonstrate as obvious subsidence on the backslope (see 'cc'). Regarding to valley regions with flat terrain (the foot of slopes), the actual motion trend from both sides can be measured as uplift (marked by 'd' and 'dd', respectively) when the deposition or heave is dominant, and vice versa, measured as subsidence (marked by 'e' and 'ee', respectively) when the thaw settlement is prevalent.

From Fig. 3, it is clear that the majority of active layers (60% to 65%) are relatively stable in a relatively short 3.5-yr observation period, in the range of -10 mm yr^{-1} to 10 mm yr^{-1}. Significant movements occur in two cases, including mountainous slopes and flat WIRP areas. The correlation between InSAR results with topography is a convincing clue for geomorphological processes, because errors from topography and atmospheric disturbances have been isolated by the SBAS algorithm. In addition, CPs cannot be existent in radar shadow or layover areas according to the extraction rule of target points. Therefore, the detected distinct uplifts in Fig. 3 are highly related to slopes processes (interpreted by the downward movements of ‘c_2’ in Fig. 4) rather than permafrost or the active layer growth under climate warming trends. Furthermore, a few isolated uplifts (with values larger than 20 mm yr^{-1}) located in high altitudinal mountains are highly related to the frost heave because of the low temperature throughout of years (interpreted by ‘a’ and ‘aa’ in Fig. 4). The remaining moderate-severe subsidence surface, with values in the range of -35 mm yr^{-1} to -10 mm yr^{-1}, corresponds to mountainous slopes or mild-terrain WRIP regions. The subsidence on backslopes is caused by the transitional movement of unconsolidated material, again due to geomorphological processes (interpreted by ‘cc’ in Fig. 4). Then, the district settlement on WRIP areas is caused by the combination of thaw settlement of the active layer as well as permafrost thawing near the permafrost table (interpreted by ‘e’ and ‘ee’ in Fig. 4).

Note that the tectonic motion in TP is not negligible, confirmed by the investigation of Cavalie et al. (2008) and Loveless & Meade (2011). The nominally interseismic GPS velocities (calibrated by a stable Eurasian reference frame) in recent years demonstrate that the tectonic movement over Beiluhe section, Hoh Xil natural reserve of TP is around 15 mm yr^{-1} in SW-NE direction (approximately perpendicular to the fight path of ALOS PALSAR). This will introduce a global subsidence contribution in LOS direction with values in the range of -7 mm yr^{-1} to -8 mm yr^{-1} in the Beiluhe site. However, as we known, the SBAS results only measure the relative displacements compared with a local reference point, and thus this homogeneous bias is not taken into consideration when the study site coverage is much smaller than 500×500 km^2.

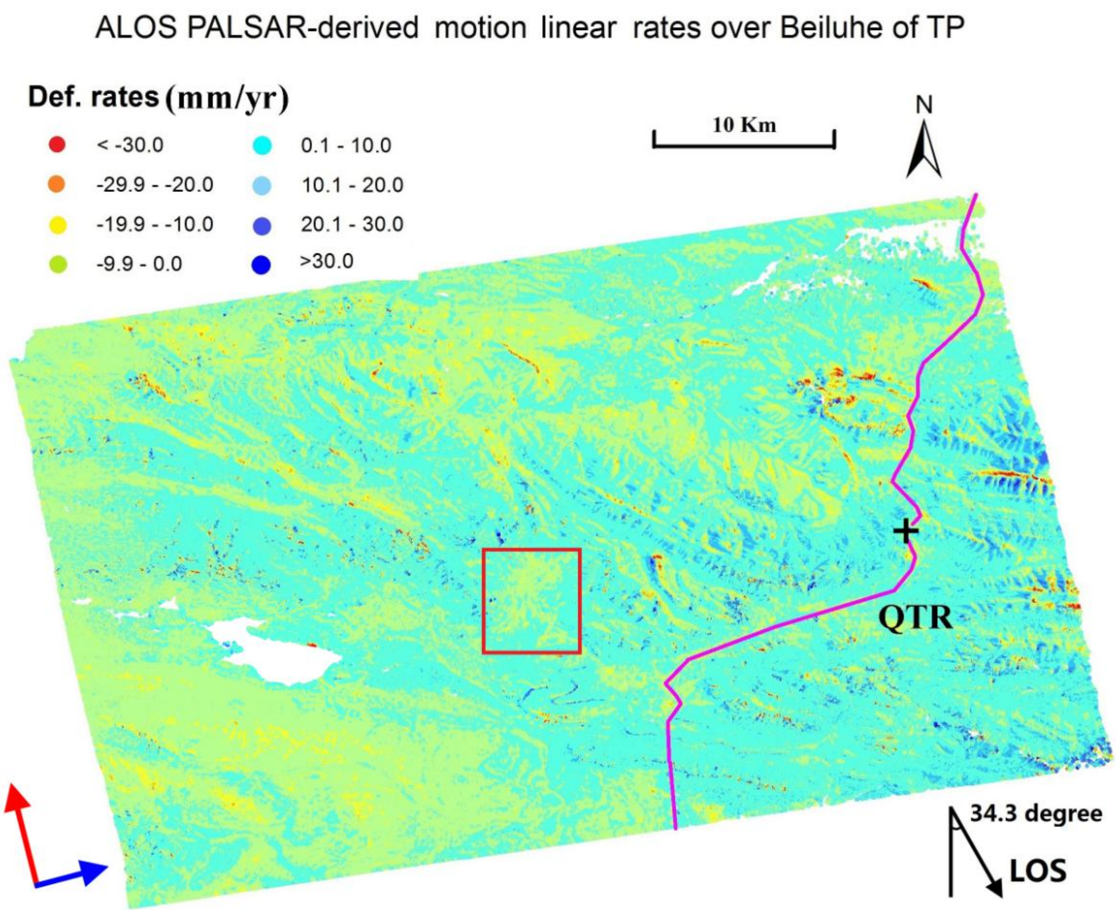

Fig. 3. SBAS-derived surface displacement linear rates over Beiluhe, Hoh Xil natural reserve of TP in LOS direction. The red rectangle represents a slope in Fenghuo Mount. The Qinghai-Tibet Railway is marked by the pink line. The cross marks the location of leveling data (nearby the Fenghuo Mount Tunnel frontier) for SBAS results validation. The satellite was travelling in the direction of the red arrow and looking in the direction of the blue arrow.

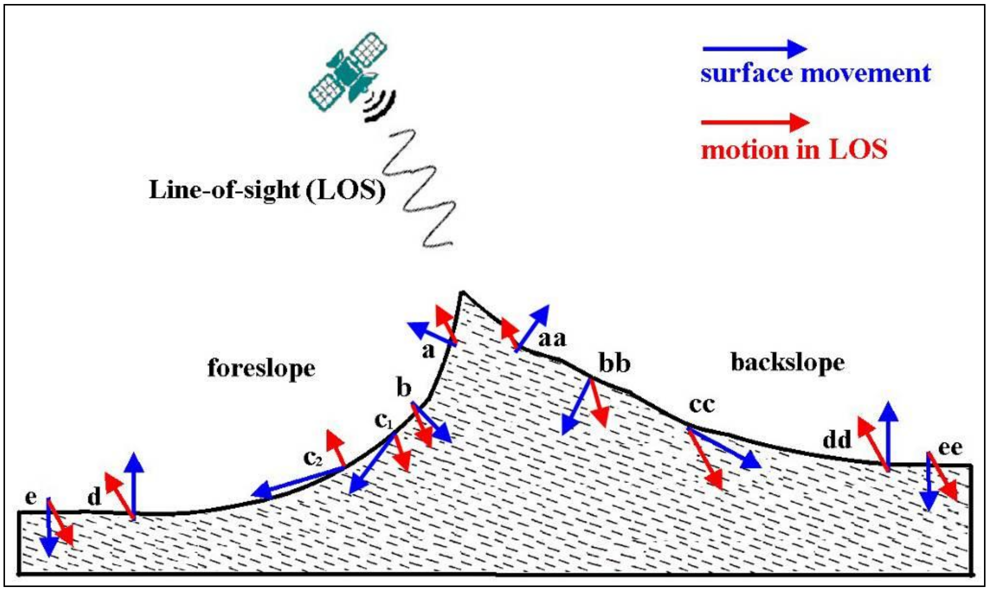

Fig. 4. The relationship between surface movements and InSAR detected displacements in LOS direction, particularly for mountainous regions.

5. Discussions

Liu et al. (2010) found that the causes of surface deformation over permafrost regions are complicated. At local scales, the deformation could be controlled by local surface vegetation, soil deposits, water/ice content, active layer thickness, hydrological settings and etc. On the other hand, the secular surface subsidence could be another driving-force due to thawing of ice-rich permafrost beneath the active layer under global warming. In this paper, the quantitative deformation discrimination of permafrost and overlaid active layer is out of scope (interested readers please refer to Liu et al., 2010, 2012); instead, from another aspect, the contributions to InSAR signals from geomorphological process and anthropogenic activities will be further discussed.

5.1 Mountainous slopes

Past field investigations indicated that the land cover in the Beiluhe site is relatively sparse, scattered by alpine meadows in flat valleys owing to the relatively higher soil moisture. In the TP arid and cold environment, the mountains are exposed by rocks or weathered deposits. Those covers are unconsolidated because of heavily decomposed rocks as well as sparse vegetation. Consequently, when the shearing force (triggered by the surface overflow and shallow groundwater flow) exceeds a threshold, a shallow-seated landslide occurs. Fig. 5 (a) shows the surface deformation field over a mountain region nearby Fenghuo Mount. Referring to relief-shaded DEM in Fig. 5(b), it is clear that uplifts in LOS direction are dominated in the upper-middle section (slope gradient > 34.3 degree) of slopes primarily owing to slope processes (can be interpreted by 'c_2' in Fig. 4). The frost heave (interpreted by 'a' and 'aa' in Fig. 4) can be another cause although its contribution is low due to the global warming trend. In the middle-lower section (slope gradient < 34.3 degree), the downward transitional movement (parallels to the bedrock beneath) is prevailing, indicating moderate-evident subsidence (interpreted by 'c_1'-'cc' in Fig. 4). The deposit accumulation is dominated at the foot of slopes, and thus derived InSAR measurements demonstrate as mild uplifts again (interpreted by 'd' and 'dd' in Fig. 4). In addition, the time series of two typical CPs (marked by 'A' and 'B' in Fig.5) is further analyzed, as illustrated in Fig. 6. The seasonal variation is remarkable, revealing the influence of southeastern Asian monsoons as well as the seasonal displacement of the active layer due to the frost heave and thaw settlement. It implies that the geomorphological process in the study site is dominant instead of permafrost evolution in a relatively short 3.5-yr observation span, particularly in mountainous areas. To make a summary, we found that physical movements along slopes are sophisticated in Hoh Xil natural reserve of TP; more information with respect to topography (slope gradients and facing direction), geology (mantle composition and surface cover), hydrology (surface-subsurface runoff and permafrost ice-content melting) are required for the active layer evolution monitoring (e.g. motion rates, directions and trends) as well as the causality interpretation (rainfall, the active layer and permafrost dynamics).

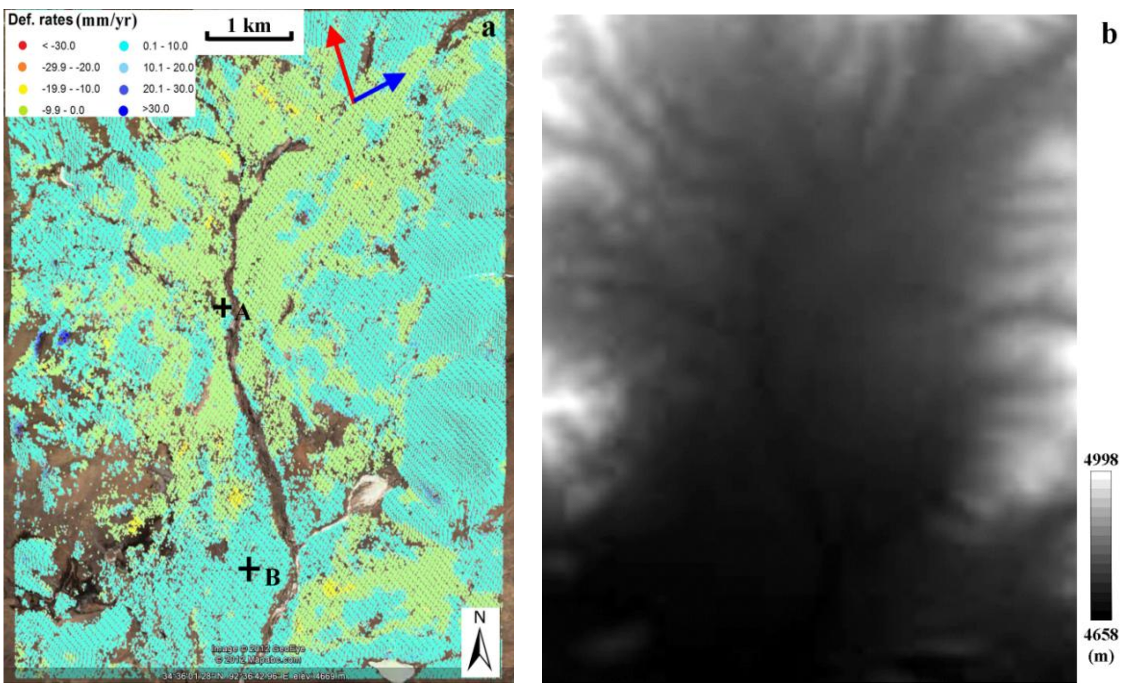

Fig.5 Different motion mechanisms can be discriminated by InSAR measurements along a mountainous area with slopes. (a) Surface deformation linear rates overlapped on the optical image from Google Earth (GE); crosses ‘A’ and ‘B’ indicate two CP targets for the time series analysis, the red and blue arrows mark the satellite travelling and looking directions. (b) Relief shaded DEM.

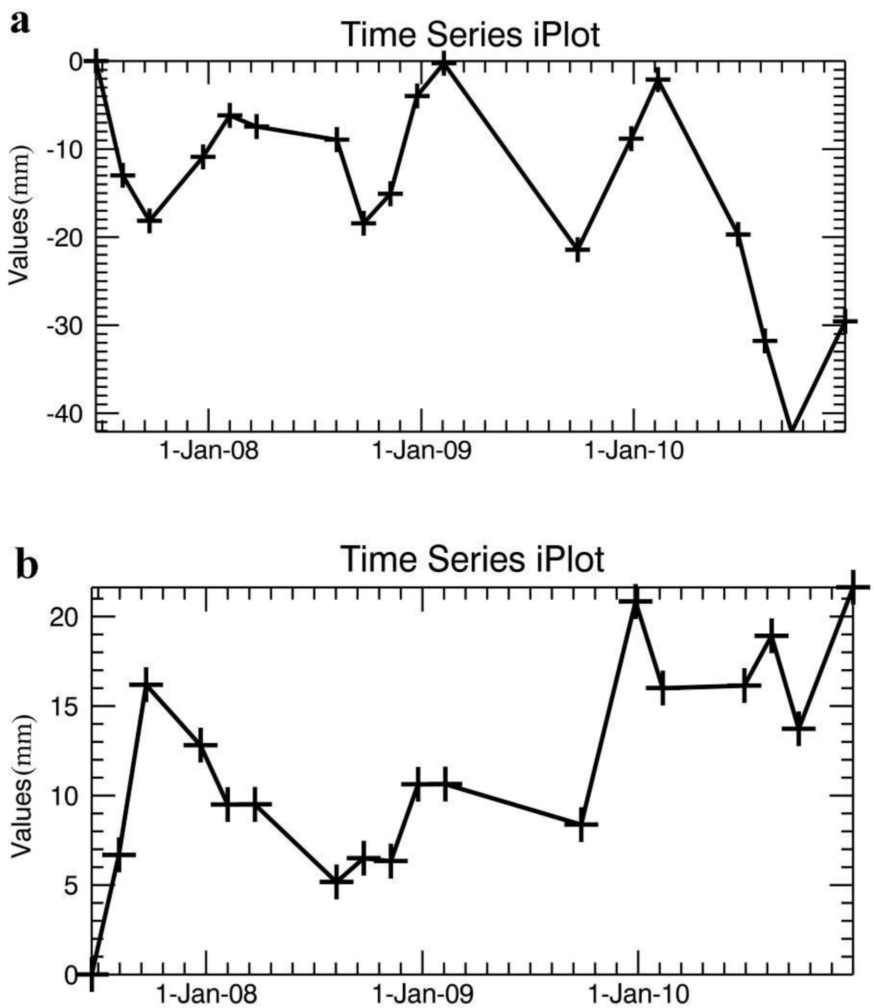

Fig. 6. Displacement time series of two typical CP targets (marked by crosses in Fig.5); (a) the subsidence, (b) the uplift. The seasonal variation is obvious.

5.2 Qinghai-Tibet Railway

The QTR project is a 100-yr grand plan; therefore its embankment instability needs to be well monitored to avoid potential geo-hazards. The embankment deformation surveillance has been covered by recent preliminary studies (Li et al., 2009; Zhang et al., 2010). In this investigation, the classical SBAS is applied considering the correlation between perpendicular baselines and acquisition times of ALOS PALSAR (Samsonov 2010); in such a way, the velocity rates noise can be further reduced primarily owing to the enhanced quality of inteferograms using the small baseline strategy, as illustrated in Fig. 7(a). Except for few uplifts due to proactive "cooling down" measures (Yu et al., 2008), see Fig. 7(b), the surface subsidence along the embankment of QTR is dominant, primarily in the range of -25 mm yr^{-1} to -10 mm yr^{-1}. This is probably caused by the combination of the increased compression settlement, destroyed active layer as well as depressed soil heat release. In general, the QTR tends to run through mild-terrain valleys considering the construction feasibility of the embankment, bringing challenges of the surface vulnerability caused by the co-occurrence of WIRP regions. Human activities, e.g. the embankment construction, easily break the original balance of the active layer, resulting in remarkable settlements from following aspects: firstly, the train-induce compression and the temperature increment of sub-surface jointly speed up the thawing settlement of the active layer in a short period (approximately 5-10 years); second, in a long-term, the secular subsidence due to thawing of ice-rich permafrost triggered by anthropogenic activities is another contribution, particularly under global warming. The motion trend of the embankment along the QTR has been exploited by the improved Interferometric Point Target Analysis (IPTA) approach in our previous study (Chen et al., 2012b). Compared with the previous one, the signal-to-noise ratio of deformation rates in this investigation have been significantly improved, resulting in easy identification for potentially risky sections, which is indeed significant for the management of the QTR embankment.

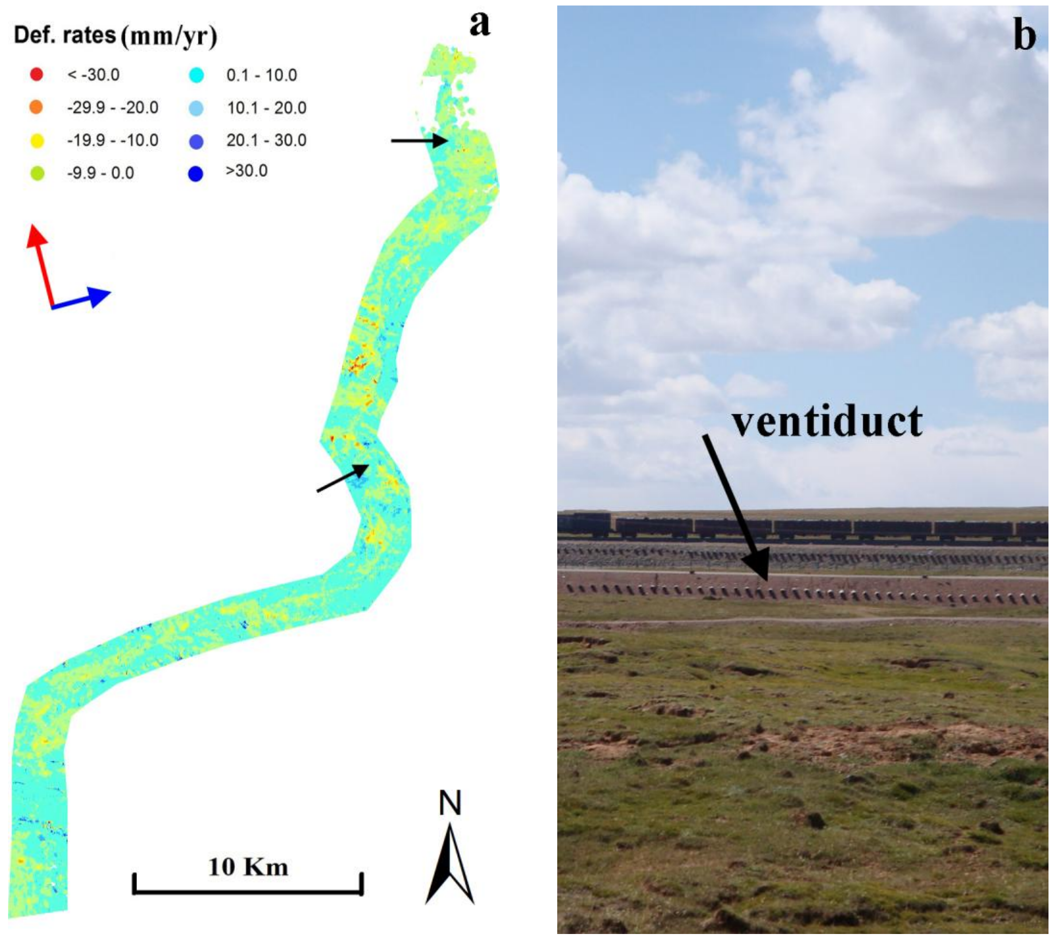

Fig.7 (a) Surface deformations along the embankment of QTR in Beiluhe section, Hoh Xil natural reserve of TP, China. The red and blue arrows mark the satellite travelling and looking directions. The uplift patches due to cooling measures are marked by black arrows. (b) Cooling-down measure of ventiduct along the embankment of QTR.

6. Conclusions

In this study, taking the Beiluhe section, Hoh Xil natural reserve of TP, China as the experimental site, we examine the relationship of the active layer evolution, geomorphological process and anthropogenic activities through InSAR approaches.

Apart from the probable tectonic activity, the SBAS derived results indicate that the movement of most active layers overlaid on the permafrost is relatively stable in a 3.5-yr short observation period, primarily in the range of -10 mm yr^{-1} to -10 mm yr^{-1} in LOS direction. In contrast, significant displacements occur in mountainous and WRIP regions. The former is highly related to the geomorphological process on those unconsolidated, weathered slope mantles triggered by seasonal monsoon heavy rainfalls. The latter is caused by the dynamics of the active layer and the permafrost beneath; under global warming, the surface over WIRP regions would be instable caused by the thawing settlement of the active layer as well as the ice-rich permafrost beneath. The main conclusions of this work can be summarized as follows.

1. Instead of PS points, the CP targets in the permafrost environment are prevalent; this phenomenon determines the feasibility of SBAS. Totally 8025313 CPs over the study site (63×45 km^2) are extracted with the temporal coherence threshold of 0.6, that is, 2800 CPs km^{-2}. Referring to the Figs. 1 and 3, it is clear that the majority of land covers are identified as DS targets, except for the water body (e.g. Beilu River) and sandy-bare ground around the Beiluhe valley because of the mirror scattering. The high density of DSs is jointly determined by the small baseline interferometric formation and L-band long wavelength of ALOS PALSAR data. In addition, the isolated interferogram clusters in the time domain (due to the corrective satellite orbit manoeuvre of PALSAR) further implies the suitability of the applied SBAS for this case study.

2. The movement of the overlaying active layer in slopes is more remarkable compared with other natural scenarios. This phenomenon is primarily determined by the erosion on unconsolidated surface triggered by heavy rainfalls in summer due to the southeastern Asian monsoons. Furthermore, the motion trend indicates a notable seasonal variation, implying seasonal thaw settlements and frost heaves of the active layer. The slopes in this arid and cold region are covered by heavily weathered mantles with bare or sparse vegetation. The stability is vulnerable under the external driving-force from intense rainfalls, resulting in landslide occurrences. The hypothesis model of surface movements in slopes has been interpreted and validated; that is, the transitional motion is dominant in the middle section, and then gradually transformed into rotational displacement due to deposits accumulation at the foot of slopes.

3. The QTR and its neighborhood are suffering from much obvious surface subsidence than surrounding features (in the range of -25 mm yr^{-1} to -10 mm yr^{-1}). This phenomenon reveals the human activity response to the evolution of the active layer as well as beneath permafrost, particularly in WIRP regions: firstly, geological conditions as well as the land cover along the embankment have been changed during the construction, resulting in aggravated active layer erosion and then remarkable surface settlements due to the thawing impact from the active layer and beneath permafrost. Second, the compression of the underlying permafrost soil has been accelerated from the downward pressure induced by the rocky foundation as well as running trains, particularly in a short-

term (within 5 years) after the QTR's operation. Last but not least, the moisture-heat balance between the active layer and air has been destroyed; resulting in thaw subsidence due to the raised sub-surface temperature, particularly under global warming.

As described in Sect. 3, in order to derive interferograms with high quality, multi-looking is applied at sacrifice of spatial resolution loss. More recently, several innovative methods (Ferretti et al., 2011; Hooper, 2008) have been proposed by synergistically using PS and DS to increase the spatial density of detected targets in natural scenarios and meanwhile preserve the original spatial resolution. Thereby, in future, those novel methods will be further investigated in the Hoh Xil natural reserve of TP, plus using high-resolution, newly-launched spaceborne SAR systems (e.g. TerraSAR-X, Cosmo-SkyMed and Radarsat-2) to extract more accurate seasonal motions and corresponding time series, taking advantages of shorter revisit cycles (Bovenga et al., 2012).

Acknowledgement. This study has been supported by funding from the Research Grants Council of the HKSAR, China (450210), the Innovation and Technology Support Programme of HKSAR, China (ITS/152/11FP), the National Natural Science Foundation of China (41201455), and Hundred Talents Program of the Institute of Remote Sensing and Digital Earth, Chinese Academy of Sciences. We thank the Associate Editor and anonymous reviewers for their constructive and insightful comments. The digital elevation model of the investigated zone was acquired through the SRTM archive. The

original ALOS PALSAR data were provided by the Japan Aerospace Exploration Agency (JAXA).

References

Berardino, P., Fornaro, G., Lanari R., Sansosti E.: (2002). A new algorithm for surface deforamtion monitoring based on small baseline differential SAR interferograms. *IEEE Transactions on Geoscience and Remote Sensing*, 40(11), 2375-2383.

Bovenga, F., Wasowski, J., Nitti, D.O., Nutricato, R., Chiaradia, M.T.: (2012). Using COSMO/SkyMed X-band and ENVISAT C-band SAR interferometry for landslides analysis. *Remote Sensing of Environment*, 119, 272-285, 2012.

Cavalie, O., Lasserre, C., Doin M.-P., Peltzer, G., Sun, J., Xu, X. and Shen Z.-K.: (2008). Measurement of intersismic strain across the Haiyuan fault (Gansu, China), by InSAR. *Earth and Planetary Science Letters*, 275, 246-257.

Chen, F. and Lin, H.: (2011). Multi-baseline differential SAR interferometry analysis of Lantau Highway, Hong Kong, using Envisat ASAR data. *Remote Sensing Letters*, 2(2), 167-173.

Chen, F., Lin, H., Yeung, K. and Cheng, S.: (2010). Detection of slope instability in Hong Kong based on multi-baseline differential SAR interferometry using ALOS PALSAR data. *GIScience and Remote Sensing*, 47, 208-220.

Chen, F., Lin, H., Zhang, Y. and Lu, Z.: (2012a). Ground subsidence geo-hazards induced by rapid urbanization: implications from InSAR observation and geological analysis. *Natural Hazards Earth System Science*, 12, 935-942.

Chen, F., Lin, H., Li, Z., Chen, Q. and Zhou, J.: (2012b). Interaction between permafrost and infrastructure along the Qinghai-Tibet Railway detected via jointly analysis of C- and L-band small baseline SAR interferometry. *Remote Sensing of Environment*,123,532-540.

Colesanti, M.: (1998). A novel phase unwrapping method based on network programming. *IEEE Transactions on Geoscience and Remote Sensing*, 36,813-821.

Ferretti, A., Prati, C., & Rocca, F.: (2000). Nonlinear subsidence rate estimation using persistent scatterers indifferential SAR interferometry. *IEEE Transactions on Geoscience and Remote Sensing*, 38, 2202-2212.

Ferretti, A., Fumagalli, A., Novali, F., Prati, C., Rocca, F. & Rucci, A.: (2011). A New Algorithm for Processing Interferometric Data-Stacks:SqueeSAR. *IEEE Transactions on Geoscience and Remote Sensing,* 49, 3460-3470.

Guo, L. D. and Macdonald, R. W.: (2006). Source and transport of terrigenous organic matter in the upper Yukon River: Evidence from isotope (delta C−13, Delta C−14, and delta N−15) composition of dissolved, colloidal, and particulate phases. *Global Biogeochemical Cycles*, 20, GB2011, 12.

Hooper, A.: (2008). A multi-temporal InSAR method incorporating both persistent scatterer and small baseline approaches. *Geophysical Research Letters*, 35, 1-5.

Hooper, A., Bekaert, D., Spaans, K., Arkan, M.: (2012). Recent advances in SAR interferometry time series analysis for measuring crustal deformation. *Tectonophysics*, 514-517, 1-13.

Hooper, A., Zebker, H., Segall, P., Kampes, B.: (2004). A new method for measuring deformation on volcanoes and other natural terrains using InSAR persistent scatterers. *Geophysical Research Letters*, 31, L23611, doi:10.1029/2004GL021737.

Immerzeel, W., Stoorvogel, J. and Antle, J.: (2008). Can payments for ecosystem services secure the water tower of Tibet? *Agricultural System*, 96, 52-63.

Ismail-Zadeh, A., Mouel, J.L.L., Soloviev, A., Tapponnier, P., Vorovieva, I.: (2007). Numerical modeling of crustal block-and-fault dynamics, earthquakes and slip rates in the Tibet-Himalayan region. *Earth and Planetary Science Letters*, 258, 465-485.

Jiang, L., Lin, H., Ma J., Kong B., and Wang Y.: (2011). Potential of small-base SAR interferometry for monitoring land subsidence related to underground coal fires: Wuda (Northern China) case study. *Remote Sensing of Environment*, 115, 257-268.

Jin, H., Yu, Q., Wang, S. and Lu, L.: (2008). Changes in permafrost environments along the Qinghai-Tibet engineering corridor induced by anthropogenic activities and climate warming. *Cold Regions Science and Technology*, 53, 317-333.

Lanari, R., Mora, O., Manunta, M.: (2004). A small-baseline approach for investigating deformations on full-resolution differential SAR interferograms. *IEEE Transactions on Geoscience and Remote Sensing*, 42, 1377-1386.

Li, S., Lai, Y., Zhang, M. & Dong, Y.: (2009). Study on long-term stability of Qinghai-Tibet Railway embankment. *Cold Regions Science and Technology*, 57, 139-147.

Lin, H., Chen, F., Zhao, Q.: (2011). Land deformation monitoring using coherent target-neighborhood networking method combined with polarimetric information: a case study of Shanghai, China. International Journal of Remote Sensing, 32, 2395-2407.

Liu, J., Wang, S., Yu, S., Yang, D., Zhang, L.: (2009). Climate warming and growth of high-elevation inland lakes on the Tibetan Plateau. *Global and Planetary Change*, 67, 209-217.

Liu, L., Zhang, T., Wahr, J.: (2010). InSAR measurements of surface deformation over permafrost on the North Slope of Alaska. *Journal of Geophysical Research, Earth Surface,* 115, F03023, doi: 10.1029/2009JF001547.

Liu, L., Schaefer, K., Zhang, T., Wahr, J.: (2012). Estimating 1992-2000 average active layer thickness on the Alaskan North Slope from remotely sensed surface subsidence. *Journal of Geophysical Research, Earth Surface,* 117, F01005, doi:10.1029/2011JF002041.

Loveless, J.P. and Meade, B.J.: (2011). Partitioning of localized and diffuse deformation in the Tibetan Plateau from joint inversions of geologic and geodetic observations. *Earth and Planetary Science Letters*, 303, 11-24.

Massonnet, D., Rossi, M., Carmona, C., Adragna, F., Peltzer, G., Feigl, K., and Rabaute, T.: (1993). The displacement field of the Landers earthquake mapped by radar interferometry. *Nature*, 364, 138−142.

Monastersky, R.: (2011). Permafrost science heats up in the United States. *Nature*, doi:10.1038/nature.2011.9681.

Niu, F., Lin, Z., Liu, H., and Lu, J.: (2011). Characteristics of thermokarst lakes and their influence on permafrost in Qinghai-Tibet Plateau. *Geomorphology*, 132, 222-233.

Qiao, X., Yang, S., Du, R., Ge, L., Wang, Q.: (2011). Coseismic slip from the 6 October 2008, Mw6.3 Damxung Earthquake, Tibetan Plateau, constrained by InSAR observations. *Pure and Applied Geophysics*, 168, 1749-1758.

Rykhus, R.P. and Lu, Z.: (2008). InSAR detects possible thaw settlement in the Alaskan Arctic Coastal Plain. *Canadian Journal of Remote Sensing*, 34(2), 100-112.

Samsonov, S.: (2010). Topographic Correction for ALOS PALSAR interferometry. *IEEE Transactions on Geoscience and Remote Sensing*, 48(7), 3020–3027.

Schuur, E.A.G., Bockheim, J., Canadell, J. G., Euskirchen, E., Field, C. B., Goryachkin, S.V., Hagemann, S., Kuhry, P., Lafleur, P. M., Lee, H., Mazhitova, G., Nelson, F.E., Rinke, A., Romanovsky, V. E., shiklomanov, N., Tarnocai, C., Venevsky, S., Vogel, J G., Zimov, S. A.: (2008). Vulnerability of permafrost carbon to climate change: Implications for the global carbon cycle. *BioScience*, 58, 701-714.

Short, N., Brisco, B., Couture, N., Pollard, W., Murnaghan, K. and Budkewitsch, P.: (2011). A comparison of TerraSAR-X, RADARSAT-2 and ALOS-PALSAR interferometry for monitoring permafrost environments, case study from Herschel Island, Canada. *Remote Sensing of Environment*, 155(12), 3491-3506.

Tarnocai, C., Canadell, J.G., Schuur, E. A.G., Kuhry, P., Mazhitova, G., and Zimov, S.: (2009). Soil organic carbon pools in the northern circumpolar permafrost region. *Global Biogeochemical Cycles*, 23, GB2023, doi:10.1029/2008GB003327.

Wang, G., Hu, H., Li, T.: (2009a). The influence of freeze-thaw cycles of active soil layer on surface runoff in a permafrost watershed. *Journal of Hydrology*, 375, 438-449.

Wang, G., Li, S., Hu, H., and Li, Y.: (2009b). Water regime shifts in the active soil layer of the Qinghai-Tibet Plateau permafrost region, under different levels of vegetation. *Geoderma*, 149, 280-289.

Wang, G., Li, Y., Wang, Y. and Wu, Q.: (2008). Effects of permafrost thawing on vegetation and soil carbon pool losses on the Qinghai-Tibet Plateau, China. *Geoderma*, 143, 143-152.

Wu, Q., Jiang, G. and Zhang, P.: (2010). Assessing the permafrost temperature and thickness conditions favorable for the occurrence of gas hydrate in the Qinghai-Tibet Plateau. *Energy Conversion and Management*, 51, 783-787.

Wu, Q. and Zhang, T.: (2008). Recent permafrost warming on the Qinghai-Tibetan Plateau. *Journal of Geophysical Research*, 11, D13108, doi:10.1029/2007JD009539.

Wu, Q. and Zhang, T.: (2010). Changes in active layer thickness over the Qinghai-Tibetan Plateau from 1995-2007. *Journal of Geophysical Research,*115,D09107, doi:10.1029/2009JD012974.

Yang, M., Wang, S., Yao, T., Gou, X., Lu, A. and Guo, X.: (2004). Desertification and its relationship with permafrost degradation in Qinghai-Xizang (Tibet) plateau. *Cold Regions Science and Technology*, 39, 47-53.

Yu, Q., Niu, F., Pan, X., Bai, Y. & Zhang, M.: (2008). Investigation of embankment with temperature-controlled ventilation along the Qinghai-Tibet Railway. *Cold Regions Science and Technology*, 53, 193-199.

Zhang, B., Zhang, J., and Qin, Y.: (2010). Investigation for the deformation of embankment underlain by warm and ice-rich permafrost. *Cold Regions Science and Technology*, 60, 161-168.